Textile Research Journal | Article

Effect of Twist, Fineness, Loading Rate and Length on Tensile Behavior of Multifilament Yarns (A Multivariate Study)

Abstract The purpose of the present study was a multivariate experimental analysis of continuous multifilament glass yarns. The experimental design involved four main factors affecting the yarn tensile behavior, namely twist, fineness, loading rate and specimen length. In the evaluation, both the main effects and their interactions were considered. In the initial test design, each factor had been covered by at least two levels. The performed analysis of variance on the constructed response surface allowed us to exclude some factors and interactions and to narrow the test design space in the second step. The interaction effect of twist and fineness could be well documented. In particular, the nonlinear effect of twist with a pronounced maximum allowed us to discuss the role of local interactions due to pressure sensitive frictional bond that gets amplified at a particular level of twist.

Key words AR-glass, interactions, multifilament yarns, tensile test, twisted yarns

Rostislav Chudoba
Chair of Structural Statics and Dynamics, RWTH Aachen University, Mies-van-der-Rohe-Str. 1, 52056 Aachen, Germany

Miroslav Vořechovský
Institute of Structural Mechanics, Faculty of Civil Engineering, Brno University of Technology, Veveří 95, 602 00 Brno, Czech Republic

Vera Eckers[1] and Thomas Gries
Institute for Textile Technology, RWTH Aachen University, Eilfschornsteinstrasse 18, 52062 Aachen, Germany

Textile fabrics are increasingly applied as a reinforcement of concrete structures in civil engineering realizations [1–3]. In this application domain, alkali resistant glass fibers and carbon fibers, as well as aramid fibers and high modulus polyethylene fibers, are used as reinforcement materials. At present, most emphasis is put on alkali resistant (AR) glass fibers, as they are comparatively cheap while having a high tenacity. Therefore, AR-glass yarns have been chosen to perform a detailed study of failure process under varied conditions. The test program was accompanied by the development and utilization of fiber bundle models [4, 5].

When applied as reinforcement, yarns are not fully penetrated by the matrix. A better bond to the matrix develops only in the outer region of the yarn cross section. Inner filaments are bonded only through the filament-filament interaction, resulting in much lower bond shear stress compared to the outer bond filament-matrix. However, as documented by Hegger et al. [6], the effect of the inner bond on the macroscopic performance of a reinforced tensile specimen cannot be neglected. While the outer bond affects the behavior at the length scale of a crack distance, the inner bond influences the failure process at the length scale of a structural element with sufficiently large stress transfer (or anchorage) length. This can be documented by a significant contribution of the inner bond to the stress level in the post-cracking regime of a tensile specimen reinforced with AR-glass yarns.

As a consequence, the interaction and damage effects for both outer and inner bond require detailed mechanical characterization. While it is possible to study and charac-

[1] Corresponding author: Institute for Textile Technology, RWTH Aachen University, Eilfschornsteinstrasse 18, 52062 Aachen, Germany. Tel: +49 241 80 95624; fax: +49 241 80 92149; e-mail: vera.eckers@ita.rwth-aachen.de

terize the interaction between a single filament and matrix experimentally [7–9], it is impossible to directly test the *in situ* filament-filament interaction. Due to the complex packing of filaments in the yarn with a high amount of irregularities, it is only possible to study the interaction effects indirectly by introducing different levels of transverse pressure between filaments in the yarn.

The idea underlying the present study was to apply twisting in order to introduce different levels of transverse pressure. The modified structure affected both the bonding level and the evolution of the damage in the yarn. In order to isolate this effect in a broader context, additional parameters were included in the experiment design, namely effects of loading rate, specimen length and filament diameter (directly linked to the fineness of the yarn). These factors have been studied in various contexts by several authors. Some related studies on involved factors are briefly reviewed.

The rate effect has been studied for several materials, namely E-glass, aramid and carbon by Zhou et al. [10]. While carbon yarns exhibited no rate effect, the response of E-glass fibers also tested here was found to be rather sensitive. The questions addressed here were (1) what is the rate effect on the applied AR-glass yarn and (2) does the rate-sensitivity also affect the studied pressure-sensitive bonding.

Specimen length has a rather complex influence on the yarn performance: besides the theoretically well described statistical size effect attributed to the flaw distribution along the bundle [11, 12], there exist additional sources of length-dependency including the filament slack [13], effect of number of filaments [14], and effect of filament length distribution [4]. These effects are well theoretically captured and explained. Therefore, it is possible to identify a range of lengths with inferior effect on yarn performance in order to focus on the effect of twist on yarn performance.

Linear density (fineness) has been included in the study due to the anticipated interaction with the twist. The data on fineness, filament diameter and material density implied the number of filaments, n, and characterized the bundle structure in its virgin state. The studied AR-glass yarns consisted of approximately the same amount of filaments at the tested levels of fineness. As a consequence, the effect of fineness could essentially be regarded as an effect of changing filament diameter. Therefore, it might be speculated that the yarn packing remained similar for all levels of fineness. On the other hand, structural effects might arise due to relative differences of filament bending stiffness and strength with respect to the applied twist level and specimen length.

As mentioned above, the other source of structural effect included in the fineness is represented by the number of filaments, n, which has been thoroughly analyzed [15, 16]. The studies performed by Vořechovský and Chudoba [5] documented that for large number of filaments with random strength, the bundle mean strength per fiber asymptotically approached constant value given by Daniels [14] connected with fast decay of coefficient of variation (strength standard deviation was proportional to the inverse square root of n) of the Gaussian strength distribution. In the present study, the number of filaments was roughly 1600, so that the effect of slight variations of n on the bundle performance should become negligible.

The effect of twist has been devised to introduce different levels of internal interaction between filaments during the loading. A classical work is the book [17] presenting a common analysis of an idealized helix-twist geometry. This model predicted that both yarn strength and stiffness were proportional to the squared cosine of the helix angle. The model assumed uniform perfectly elastic filament properties with a sudden failure. A more sophisticated treatment in the book took into account the transverse forces and the lateral contraction. We remark that these models are deterministic and there is no treatment of the interaction between filaments upon breakage.

Fully statistical theory for the strength of twisted bundles has been formulated using the strain-based fiber bundle model [13] by incorporating the fiber helical paths [18]. However, the theory also excluded fiber interactions such as friction between fibers which is, in reality, strongly strengthened by lateral compression in highly twisted yarns. This effect has been theoretically well documented by Pan et al. [19] using a model including fragmentation. The increased inter-filament bond was included using the chain of fiber bundle models of the critical length representing the stress transfer length needed to recover the filament force. Verbal description of the fragmentation process has been presented by Broughton et al. [20] on a particular example of a surface treatment strongly affecting the yarn performance.

The fragmentation process has been thoroughly studied using a stochastic model [21] reflecting the effect of changing lateral pressure due to twist and its affect on the load-sharing between broken and surviving filaments. The numerical study was related to tests on pseudo-filament-yarns with filaments represented by component yarns (cotton and polyester). Using the designed pseudo-yarns, the model could be validated in terms of its ability to propagate the component behavior (pseudo-filaments) to the structural behavior (yarn).

A comprehensive experimental study of twisted continuous glass yarns has been presented by Jones et al. [22]. In this study, no increase of yarn strength due to twist was observed. As a consequence, the data could be well reproduced by the classical interaction-free models presented by Hearle et al. [17]. The same holds for tests of glass/nylon blended continuous yarns presented later in [23]. The authors reported tenacity and modulus decrease with increasing twist level, while gaining greater total elongation-to-break and less "kinky" behavior. On the other

hand, a strength increase up to an optimum twist level has been observed in tests on polymeric yarns by Rao and Farris [24]. However, this work was primarily focused on improved reflection of the apparent yarn stiffness (effective tensile E-modulus).

Summarizing, it was unclear from the reviewed literature whether or not the twisting of studied AR-glass yarns could lead to strength increase due to higher bond with associated fragmentation. While it was not reported by Jones et al. [22], it should be, at least in some range of twist levels, observable according to Pan et al. and Realff et al. [19, 21].

In order to clarify this issue experimentally in a general context, a complex testing program has been prepared and analyzed using the methodology of Design of Experiments [25]. The above discussed test parameters have been varied simultaneously and not on the one-at-a-time basis. This approach allowed us to justify the constructed response surfaces based on their statistical significance. Similar strategy has been followed in a multivariate study on cotton yarns [26] using the multivariate statistical technique based on principal component analysis for explanation of variance and covariances of measured parameters. By applying the multivariate experiment design, we intended to localize the range factors with pronounced effect on pressure sensitive filament-filament bonding. The present paper is to be regarded as a stepping stone for micro-mechanical characterization of the local interaction that shall be performed in further publications. Here, the focus is on a detailed description of the test results and their phenomenological interpretation.

In the next section, the experimental set-up with the adjustable parameters is described. Following that, the experimental design is described and the results are presented in form of response surfaces and discussed.

Test Setup

A tensile testing machine Z100 of Zwick Roell Gruppe, Ulm, was used for the experiments. It works motion controlled meaning that the testing speed was set in advance and the resulting forces were measured. The tensile force was determined with a load cell at the upper clamping and transformed to nominal stress as:

$$\sigma = \frac{F}{A} \tag{1}$$

with A representing the actual cross-sectional area of the yarn calculated by dividing the linear density (e.g. 2400 tex) by the density of AR-glass: $A = 2400[\mathrm{g}]/1000[\mathrm{m}]/2.678[\mathrm{g/cm^3}] = 0.896\ [\mathrm{mm^2}]$. This area corresponds to the total area of all filaments ($A = n \times A_1$, where $n \approx 1600$ is the number of filaments in the yarn and $A_1 = \pi d^2/4$ is the cross sectional area of one filament, see Table 1 for the diameter d paragraph 9). The nominal stress is used for comparison purposes of apparent yarn performance under various conditions and does not reflect changes at structural level, such as the fiber volume fraction. The strain was obtained by dividing the control displacement by the clamp distance:

$$\varepsilon = \frac{u}{L} \tag{2}$$

Loading velocity could be varied within the range from 2.5 to 200 mm/min.

Specimen ends were embedded in epoxy resin to prevent slippage and damage of filaments during testing. The preparation of the specimens was performed using rubber molds. The yarn was put into the mold and straightened under light tension. At the designated location, the epoxy blocks were cast as shown in Figure 1. The curing time of the epoxy resin was 24 hours. The relatively low modulus of epoxy resulted in a gradual transfer of loading into the filaments preventing their brittle failure in the clamping. The resin used for the load introduction was the epoxy resin EP210 together with the hardener EPH412-2. It has a Young's modulus of 3.250 GPa, a tensile strength of 63MPa and a maximum strain of 8.7 %. The length of the blocks was 75 mm, their width and thickness were 8 mm. The ends of the yarns were embedded in separate molds, so that the length could be arbitrarily adjusted up to the maximum distance of the jaws of the testing machine (approximately 500 mm).

The introduction of twist was a crucial aspect of the specimen preparation. Both manual and automated twisting has been applied. In the former case, the specimen was fixed at the upper jaw of the machine and manually twisted at the bottom end and then fixed in the jaw. In the latter case, industrially produced spun yarns delivered on the bobbins were tested. The automated twisting was performed under light pre-stress stabilizing the production process. The preliminary tests on the industrially twisted yarns indicated high level of initial damage that totally drowned the effect of twist on the overall yarn strength. For this reason, the manual twisting without pre-stressing was chosen for the present study. In view of this study, the technology was not of primary interest, the focus was on the reproducibility of the studied effects. The additional manual effort was negligible.

Visual impression was that the twist level was not uniform over the yarn length, especially in the case of high twist levels. The helix length varied rather strongly in the range 2–10 cm, see Figure 1 top right for illustration. The reason is probably an irregular structure of multifilament yarn including non-uniformity of lengths. This fact should be kept in mind when modeling the yarn response, as it would induce scatter of *in situ* filament-filament interaction along the yarn.

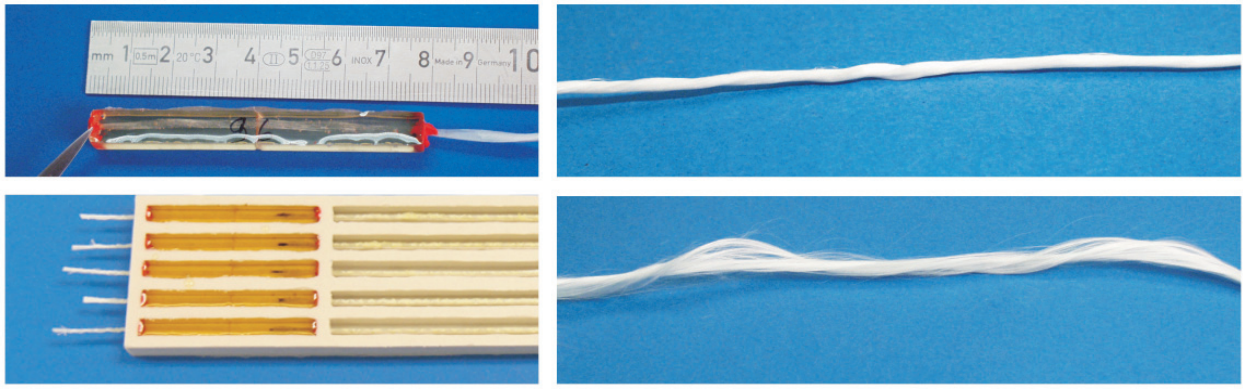

Figure 1 Preparation of the specimens. Left: epoxy-resin blocks and rubber molds for casting. Right: highly twisted specimen before (top) and after (bottom) tensile test.

Table 1 Characteristics of tested yarns: finenesses and nominal filament diameters.

Nominal fineness	Measured fineness	Filament diameter
[tex = g/km]		d [μm]
640	646	14
1200	1270	19
2400	2450	27

The tested material was AR-glass yarn (in particular the roving named CemFIL Direktroving LTR5325, produced by Saint Gobain Vetrotex). The weight fraction of sizing was approximately 0.8 %. The yarn was delivered with three nominal finenesses (640, 1200, 2400 tex). Table 1 summarizes the actual values of fineness obtained by weighting the yarn segments and the nominal filament diameters.

Experiment Design

The goal of the study was to capture the effect of twist in combination with other possible interacting effects on the total performance of the bundle. In particular, the multivariate study was performed with the goal to identify the range of tested parameters with evidently positive effect of transverse pressure on the increased bond performance and to make the trends in the response change evident in terms of the statistical design of experiments. The considered interacting factors were the twist level (**A**), loading rate (**B**), specimen length (**C**) and fineness (**D**).

The yarn response was characterized by two variables obtained from the stress-strain diagrams: the peak stress, σ_{max}, and peak material stiffness, E_{max} (see Figure 2):

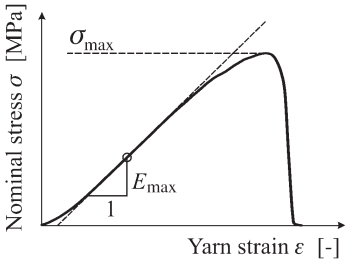

Figure 2 Typical stress-strain diagram with characteristic response variables.

$$E_{max} = \max \frac{d\sigma}{d\varepsilon} \tag{3}$$

The chosen levels of the four input factors are given in Table 2. Also specified is the number of runs performed for each combination of levels. In order to reduce the total number of tests the experiment design was constructed in two steps. In the first phase (design I), 200 tests were conducted with all four factors varied at up to four levels (twist) in order to identify/exclude interactions and to construct the initial response surfaces.

Based on these results, a further 102 tests (design II) were performed within an adjusted design space reduced to two dimensions (twist and fineness). Further, the tested range of twist was narrowed to the range capturing the maximum effect on the yarn strength with the goal to confirm the shape of the response surface.

The chosen levels of tested factors (**A–D**) were set based on the following considerations:

A: Twist was introduced manually with one end of the specimen clamped in the upper jaw of the test machine.

Table 2 Summary of the experimental design: numbers of realizations for each factor combination. Numbers in parentheses denote experiments belonging to the refined design (II). The six stars denote six censored outliers.

B: Strain rate [%/min]	**D:** Fineness [tex]	**C:** Length [mm]									Σ	
		250				500						
		A: Twist [turns/m]										
		0	20	40	60	0	10	20	40	60		
1	640	2	2*		11	8			5		28	73
	1 200	7				1				6	14	
	2 400	6		6	3	6		2		8	31	
8	640	7		1						7	15	41
	1 200			3		1		5			9	
	2 400	2			7*	6				2	17	
40	640	7		5	4	7 (6)	(10)	(10*)	(10*)	10	33 (36)	86 (102)
	1 200	1	1		6	6	(10)	(10)	1 (10)		15 (30)	
	2 400	11			8*	6 (6)	(10)	(10*)	6 (10)	7	38 (36)	
Σ		43	3	15	39	41 (12)	(30)	7 (30)	12 (30)	40	200 (102)	
		100				100 (102)						

The lower end was twisted up to the prescribed level [turns/m]. The design included 0, 20, 40, 60 turns/m. An additional twist level of 10 turns/m was added in the refined design (II).

B: **Loading rate** was imposed at three levels: 1, 8 and 40 %/min. The small rate represented the lower bound of loading rates appearing in structural composite elements. However, it was necessary to include higher rates introduced by the damage process of the composite material, namely by the rate of fracture propagation in a crack bridge. The applied test setup allowed us to reliably cover the rate range with upper level set to 40 %/min.

C: **Specimen length** was tested at two levels (250 and 500 mm) in order to ensure that there was no strength reduction due to imperfections of filament fixing at the clamps and due to filament slack. As documented on an example of AR-glass yarn 2400 tex [4], these effects vanished on specimens longer than 100 mm. The second source of strength reduction, namely the statistical size effect in the sense of the weakest-link model was thoroughly tested and described for the tested material in the chosen range of lengths [5]. Based on these studies, the two lengths were chosen primarily in order to capture interactions of length with the other factors.

D: **Fineness** could only be varied within the levels available commercially. The studied vetrotex yarn was available with 320, 640, 1200 and 2400 tex. The 320 tex yarn was not tested since it differed in the production technology; it was produced by halving the 640 tex yarn. As apparent from Table 1, the variation of fineness induces in fact a variation of filament diameter, since the (approximate) number of filaments $n = 1600$ was identical for all fineness levels.

Since the chosen number of levels varied for each factor, it was impossible to choose a standard design so that the general *D-optimum* design for constructing the response surfaces by linear regression was used [25]. As the testing was performed over several days, the order of test runs was randomized with the goal to minimize errors due to uncontrollable factors.

Results and Discussion

Design I

The normalized yarn strength obtained for all the combinations of levels is summarized in Table 3 in terms of the mean and standard deviation. The corresponding response surface is shown in Figure 3 visualizing the approximation (σ_0, …, σ_{10} are the regression coefficients)

$$\begin{aligned}\sigma_{max} = {} & \sigma_0 \\ & + \sigma_1 A + \sigma_2 B + \sigma_3 C + \sigma_4 D \\ & + \sigma_5 A^2 + \sigma_6 D^2 \\ & + \sigma_7 A^3 \end{aligned} \Bigg\} \text{main factors}$$

$$+ \sigma_8 AC + \sigma_9 AD + \sigma_{10} BC \Big\} \text{interactions} \qquad (4)$$

where $\{\sigma_0, \ldots, \sigma_{10}\} = \{+1450.09; -371.11; +92.09; +5.86; -145.54; -302.43; -141.82; +344.85; +42.93; -120.24; +20.28\}$. The coded factors A–D map linearly to levels **A–D** summarized in Table 2. Besides the surface, the figure

Table 3 Yarn strength σ_{max} statistics: mean (standard deviation).

B: Strain rate [%/min]	**D:** Fineness [tex]	**C:** Length [mm] 250 — **A:** Twist [turns/m] 0	20	40	60	**C:** Length [mm] 500 — **A:** Twist [turns/m] 0	10	20	40	60	Σ	
1	640	1060.322 (28.045)	1268.56 (0)		1094.455 (134.443)	885.779 (49.979)			1205.77 (76.415)		1057.159 (155.752)	
	1200	1090.93 (94.138)				1194.557 (0)				1076.216 (31.615)	1092.026 (75.617)	959.439 (207.678)
	2400	981.158 (85.357)		848.189 (68.664)	636.679 (26.619)	882.762 (110.265)		1196.758 (100.007)		583.972 (65.181)	814.451 (197.952)	
8	640	1086.39 (42.153)		1358.126 (0)						1269.255 (143.474)	1189.843 (142.341)	
	1200			1368.614 (127.104)		1271.915 (0)		1482.015 (115.305)			1420.87 (134.996)	1096.563 (278.042)
	2400	1042.477 (94.261)			690.219 (70.028)	928.995 (79.538)				713.402 (41.734)	826.69 (154.51)	
40	640	1208.814 (68.552)		1407.752 (91.601)	1255.735 (47.075)	1078.345 (89.823)	1302.001 (92.684)	1338.897 (92.535)	1433.823 (97.106)	1451.17 (78.645)	1298.927 (157.611)	
	1200	1286.854 (0)	1665.222 (0)		1168.132 (82.188)	1240.072 (71.68)	1470.266 (79.395)	1579.019 (82.264)	1488.14 (105.551)		1428.082 (170.204)	1242.055 (224.586)
	2400	1070.517 (74.942)			765.67 (72.647)	1011.7 (75.663)	1268.03 (71.906)	1306.629 (114.357)	1085.353 (126.754)	880.709 (79.926)	1072.866 (185.51)	
Σ		1089.722 (102.458)	1466.891 (198.331)	1172.791 (280.039)	958.967 (240.491)	1019.293 (142.2)	1346.766 (120.443)	1411.529 (159.737)	1284.596 (210.462)	1052.933 (331.981)	1153.65 (258.39)	
		1060.469 (222.078)				1199.069 (262.629)						

shows the coverage of the design space in form of data points located at each tested parameter combination; compare with Table 2.

The significance level of the studied effects was evaluated using the standard procedure of analysis of variance (ANOVA) [25, 27]. The evaluation was based on comparing the variance of the data with respect to the model (equation (4)) to the variance with respect to a reduced model. In simple terms, we tested whether or not the trends proposed by the model could be the result of noise (null hypothesis). If this hypothesis could be rejected at the required significance level the trends were considered to be evident. In our case, ANOVA identified all terms in equation (4) as strongly evident, except for the factor *C*. Further, the interaction *BC* was classified as less evident, since the ranges of measured values partially overlapped. Furthermore, using ANOVA two outliers could be detected. Subsequent visual inspection of the specimens confirmed production errors so that these tests were discarded from the design.

The obtained response surface (equation (4)) contained only the significant effects and interactions. Evaluation of the main effects showed a nonlinear (cubic) effect of twist (**A**). The effect of loading rate (**B**) was assessed significant for linear term, but not for the quadratic one. The obtained rate dependency corresponded with results presented for E-glass yarns [10]. As desired, the effect of the specimen length (**C**) turned out to be insignificant, which meant that the statistical size effect was negligible in the tested length range. However, its effect had to be retained in the analysis due to the interaction of length with the twist level. The main effect of fineness (**D**) was evaluated as quadratic.

Interactions that turned out to be statistically insignificant were **AB** (twist and loading rate), **CD** (length and fineness) and **BD** (loading rate and fineness). The most significant interaction was detected for **AD** (twist and fineness). Their dominating effect within the four-dimensional test space is visualized in form of six surfaces over the interacting factors **AD** at all level combinations of **BC** i.e. loading rates in rows and lengths in columns (see Figure 3).

Before focusing on the **AD** interaction in detail, we have to address a somewhat suspicious result concerning the interaction identified between **BC** (loading rate and length). Comparison of the isolines in two bottom surfaces of Figure 3 revealed an inverse length effect for rapid loading (40 %/min). This would suggest a hardly acceptable conclusion saying that the more flaws along the yarn are available (longer specimens) the stronger the "healing" effect of the increased loading rate. Even though this trend was assessed as less significant in terms of ANOVA compared to the other listed effects, it cannot be simply clarified and requires further investigation.

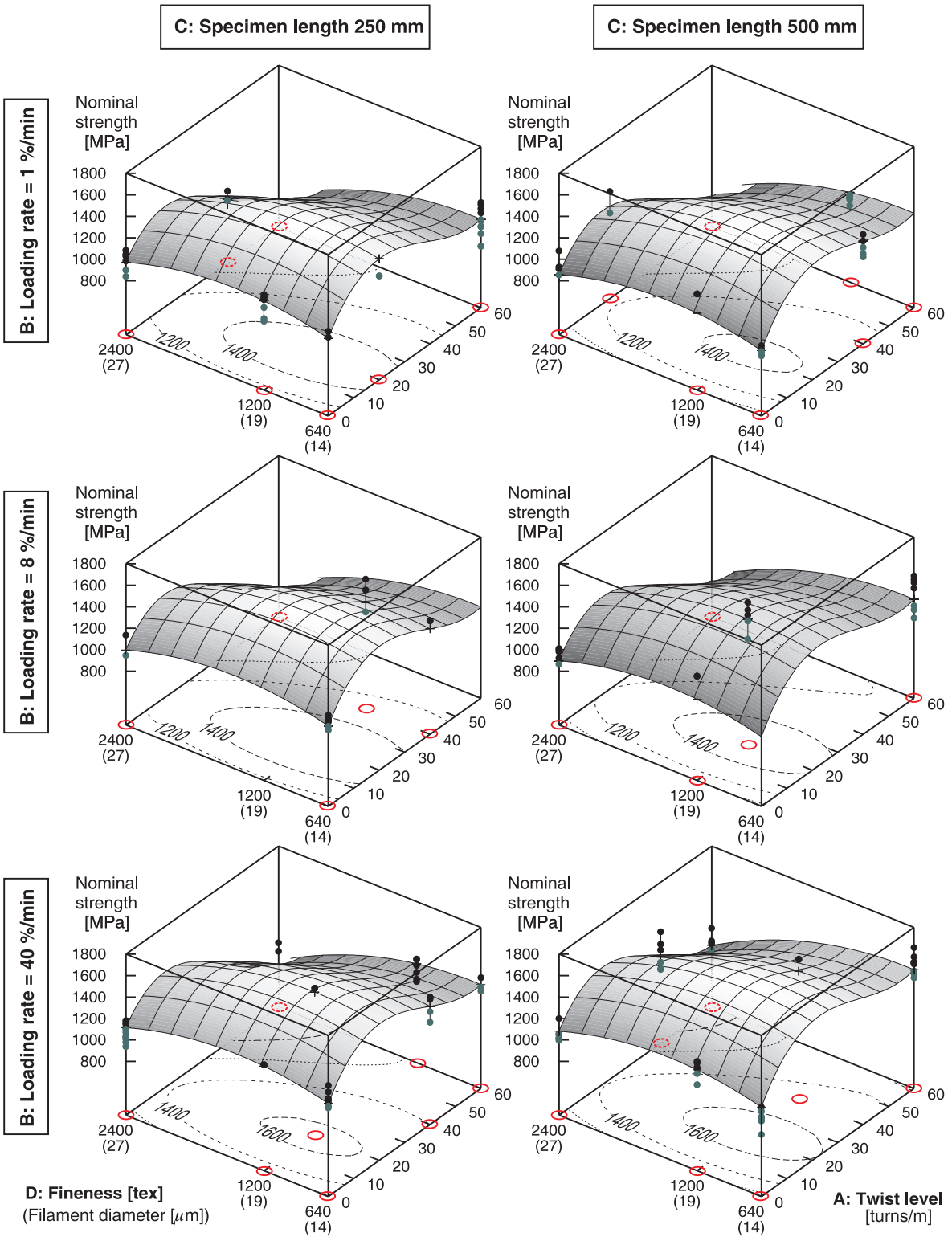

Figure 3 Yarn tensile strength σ_{max} in design I: measured data and response surface.

Using Figure 3, it can be concluded that the shape of the response surfaces was similar for all combinations of length and loading rate. Moreover, the contour lines revealed that the maximum strength was achieved for the combination with the same twist (20 turns/m) and fineness (1200 tex) independently of the loading rate and length. This result suggests that with the present experiment design we were able to isolate a general effect of strength increase for moderate number of turns/m (0–20) with subsequent strength reduction for higher twist levels.

Design I+II

While design I was mainly prepared for a qualitative screening of the studied parameter space, the second design was arranged with the goal to confirm the main effects and interactions with more focused resolution of twist levels: 0, 10, 20 and 40 turns/m (see Table 2). The levels of loading rate and specimen length were fixed to 40 %/min and 500 mm, respectively. This was justified by the low interactions of these factors with the twist and fineness (similar shape of the response surfaces in Figure 3). The analysis of variance detected three outliers that were censored after visual inspection, see Table 2. The strength response surface resulting from the merged design I+II is shown from two viewpoints in Figure 4. The figure contains the almost identical surfaces both for design I and design I+II. The surfaces did not differ in the structure of the approximation (see equation (4)), but differed slightly in the regression coefficients. Their difference is indicated by the isolines in the **A–D** plane. Apparently, the inclusion of the new data in the approximation did not change the response surface significantly, so that it could be concluded that design II confirmed the trends and the champion specimen was identified for the combination (**A** = 20 turns/m, **D** = 1200 tex).

Interpretation of the Response

Two main questions required addressing in the phenomenological interpretation of the results: what were the reasons for the continuous strength increase in the range 0–20 turns/m and for its reduction at higher twist levels. These aspects can be discussed with the help of the stress-strain diagrams shown in Figure 5 in two different views. While the first row allows the reader to qualitatively compare the shapes of stress-strain diagrams for the pairs of twist 0 and 20 (left) and 0 and 60 (right) turns/m, the second row completes the picture by showing the full set of measured curves for 20 and 60 turns/m.

Comparing the stress-strain diagrams for the twist levels **A** = 0 and 20 in Figure 5 left, we observed that for the non-twisted reference yarns, there was a higher amount of slack (delayed activation) than for **A** = 20 turns/m. This meant that raw yarns had production-induced waviness and that the differences in the filament length due to this waviness got reduced at moderate levels of twist.

The second feature of the stress-strain diagram to note is that for non-twisted yarns filament breakages were spread

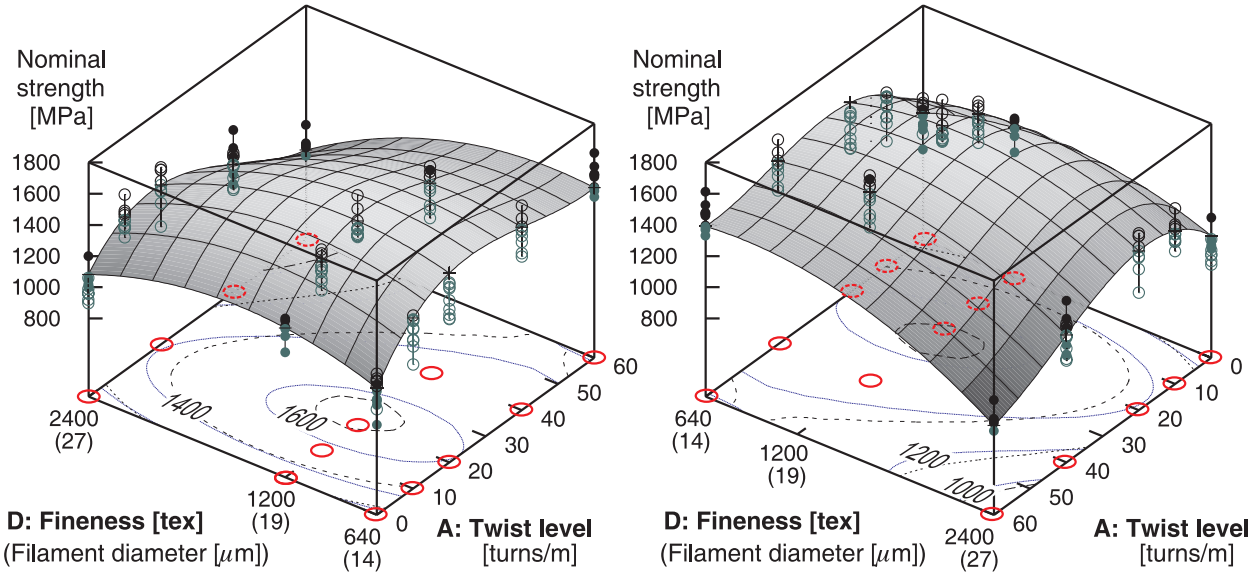

Figure 4 σ_{max} (design I+II). For the combination: rate = 40 %/min and length = 500 mm. Empty circles: points belonging to design II. Continuous isolines: design I (compare with new dashed isolines for design I+II). Black and green data points are above and below the surface, respectively.

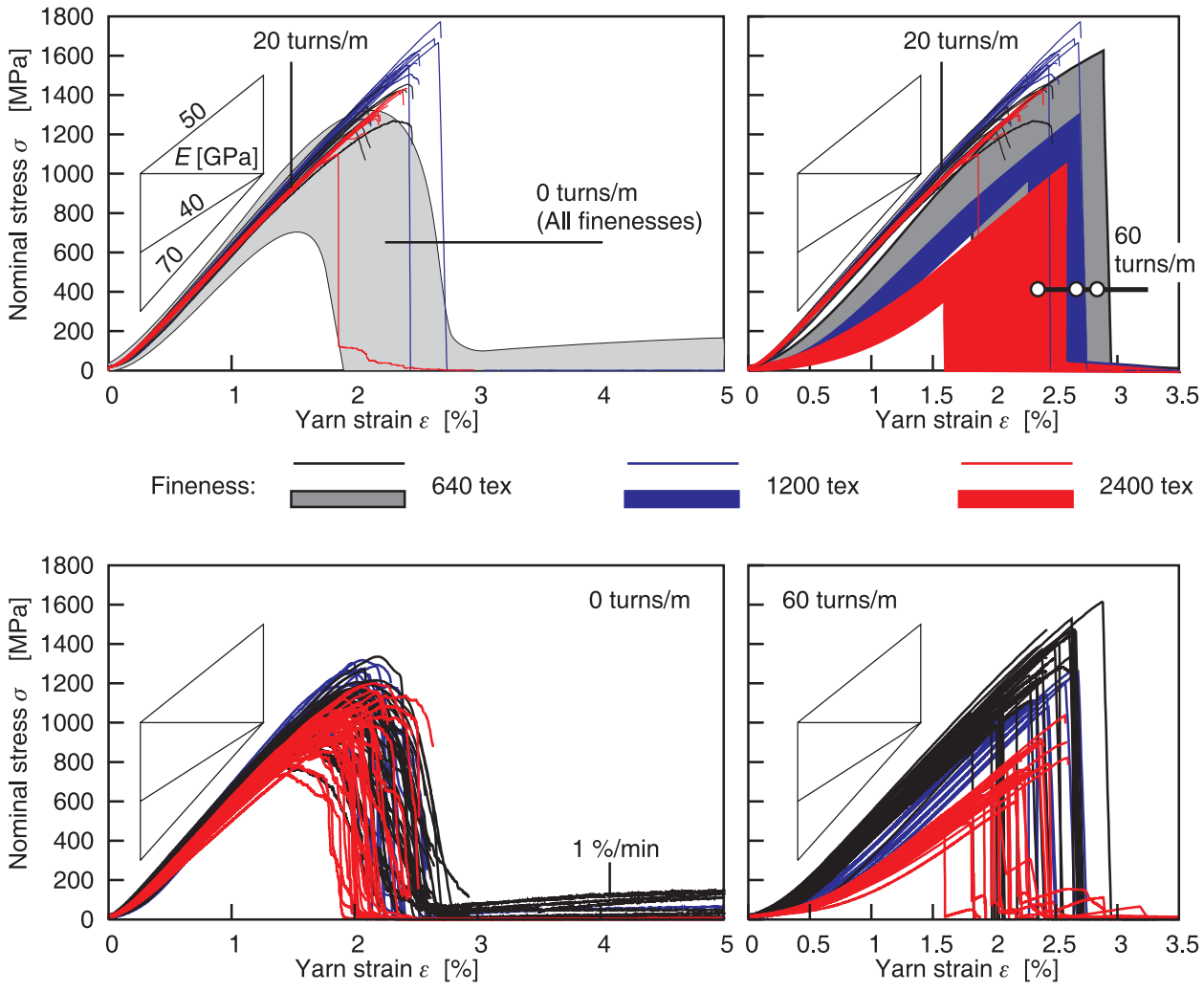

Figure 5 Stress-strain diagrams. Top row: 20 turns/m compared to envelopes of zero twist level (left, all finenesses) and 60 turns/m (right, distinguished finenesses). Bottom row: detailed view on zero twist level (left) and 60 turns/m (right).

over a wide range of nominal strain. This indicated independent failure of filaments in conjunction with a high scatter in filament breaking strain. Visually, the specimens failed with filaments randomly breaking along the yarn without localization at some cross section. The random distribution of breaks along the yarn led to a high internal friction in the post-peak range.

Third, in contrast to the non-twisted yarns, the twist level 20 turns/m led to a simultaneous failure of all filaments at significantly higher stresses followed by a sudden localized failure. The only explanation for this increase was a strong interaction between the filaments (local load sharing). In our opinion, the mentioned reduction of waviness due to improved filament packing could not sufficiently explain the homogeneous behavior of the bundle. The amount of scatter in breaking strain did not vanish for the twisted yarns. Therefore, the filament breakages at the high stress level must have been compensated by the inter-filament bonding. Such a scenario would correspond to the fragmentation discussed by Pan et al. [19]. This issue shall be clarified in the future, both experimentally and using numerical models.

In Figure 5 top-right, the opposite tendency in strength evolution is shown on the example of the twist levels 20 and 60. The amount of slack got very large for twist level 60, indicating high irregularity in the yarn packing leading to an increased structural influence of twist. On the other hand, these specimens also exhibited a sudden failure (Figure 5 right), indicating a high amount of interaction. In view of the studies presented by Chudoba et al. [4] for

Table 4 Statistics of maximum achieved yarn stiffness E_{max}: mean (standard deviation).

B: Strain rate [%/min]	**D:** Fineness [tex]	**C:** Length [mm] 250 — **A:** Twist [turns/m] 0	20	40	60	**C:** Length [mm] 500 — **A:** Twist [turns/m] 0	10	20	40	60	Σ	
1	640	68.811 (0.809)	65.836 (0)		62.103 (2.11)	70.561 (0.567)			67.885 (1.326)		66.315 (3.972)	62.031 (8.599)
	1200	69.237 (2.959)				74.133 (0)				63.518 (1.834)	67.136 (4.139)	
	2400	62.677 (3.501)		51.332 (3.312)	44.205 (0.617)	67.574 (2.073)		67.395 (0.127)		47.369 (1.851)	55.995 (9.278)	
8	640	68.59 (1.351)		67.593 (0)						67.073 (0.968)	67.816 (1.352)	64.114 (9.444)
	1200			66.257 (2.235)		76.804 (0)		71.599 (0.944)			70.397 (3.639)	
	2400	64.211 (1.954)			44.609 (0.984)	69.483 (1.496)				50.402 (0.901)	57.111 (11.39)	
40	640	70.788 (1.248)		67.534 (0.631)	66.744 (2.561)	71.627 (1.136)	71.91 (0.672)	70.429 (1.247)	68.711 (0.732)	67.813 (0.814)	69.863 (2.106)	67.149 (5.989)
	1200	72.339 (0)	71.449 (0)		62.472 (2.055)	74.255 (0.698)	71.133 (0.443)	70.105 (1.083)	67.606 (1.399)		69.338 (3.577)	
	2400	65.824 (1.584)			46.749 (1.446)	69.308 (1.107)	69.697 (0.523)	67.347 (0.686)	62.654 (1.226)	52.27 (0.652)	63.256 (7.385)	
Σ		67.414 (3.474)	68.643 (2.806)	60.802 (8.095)	55.472 (9.049)	70.682 (2.392)	70.913 (1.071)	69.538 (1.839)	65.95 (2.924)	59.36 (8.606)	65.494 (7.564)	
		61.862 (8.789)				67.265 (6.155)						

zero-twist, this was unexpected since the spread in filament activation should lead to the spread in the filament failure on the first-come-first-go basis. The discrepancy could be explained by irregular packing of filaments due to over-twisting the yarn into compact and loose segments along and across the yarn (comp. Figure 1 right). While the loose segments explained the slow filament activation, the compact segments caused the brittle localized failure. This behavior might correspond to the wrapped ribbon packing described by Hearle et al. [17].

Even though the main effect of loading rate was significant, the qualitative shape of the stress-strain diagrams in Figure 5 remained the same for almost all rate levels. The only difference could be observed for zero-twist yarns (640 tex) loaded at 1 %/m, that showed a residual force after reaching the peak stress (see branches at the left hand side, bottom).

Another important characteristic of the test response was the maximum achieved yarn (structural) stiffness E_{max} (see Figure 2). It could be used to assess the maximum amount of simultaneously activated filaments during the loading history. The results summarized in Table 4 and Figure 6 left indicated that for moderate twist levels, the maximum material stiffness approached the E-modulus of glass (70 GPa). This meant that at least for some nominal strain all filaments contributed to the stress transfer with their true E-modulus. For maximum twist level, the amount of activated filaments got significantly reduced, as can be seen from Figure 6 right. This was related to the high amount of slack and supported the interpretation of the failure process discussed in the previous paragraph. The fineness influenced the material stiffness in the range (68–72 GPa) as a weak quadratic main effect.

$$\left.\begin{aligned} E_{\max} &= E_0 \\ &+ E_1 A + E_2 B + E_3 C + E_4 D \\ &+ E_5 A^2 + E_6 D^2 \end{aligned}\right\} \text{main factors}$$
$$\left. + E_7 AD + E_8 CD + E_9 BD \right\} \text{interactions} \qquad (5)$$

where $\{E_0, \ldots, E_9\} = \{+67.13; -5.86; +1.03; +1.84; -4.94; -2.02; -2.13; -3.41; +0.74; +0.96\}$.

By comparing the left hand side of Figure 5 bottom (zero twist level) with the right hand side (60 turns/m), one can see that non-twisted yarns were relatively insensitive to fineness. Still, equation (5) indicates quadratic effect of fineness and one can see this trend visually in Figure 6 left.

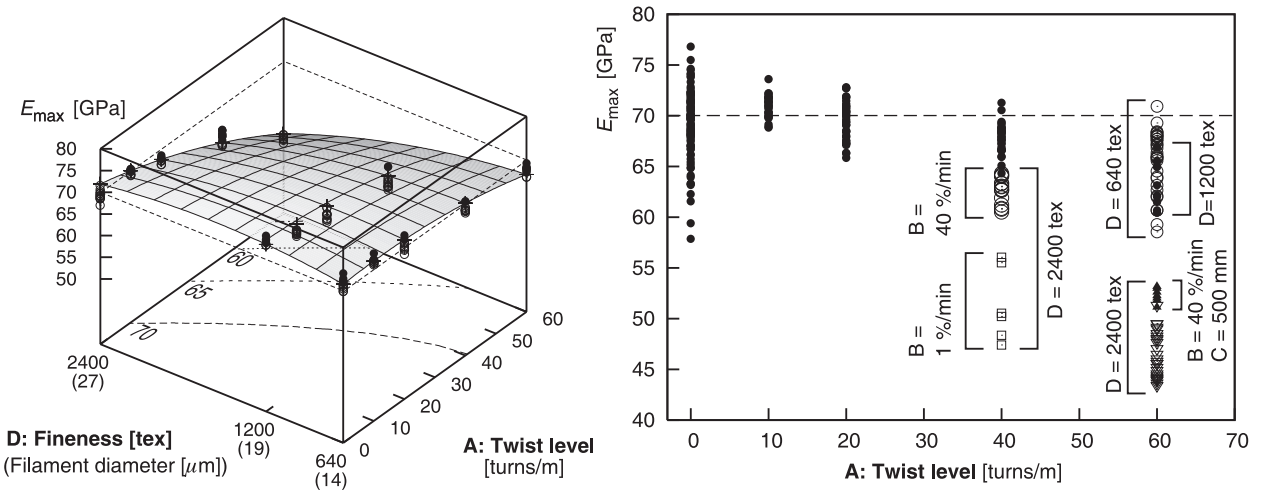

Figure 6 *E*-modulus (design I+II). Left: rate = 40%/min and length = 500 mm. Right: all data with designated clusters.

Indeed, the surprising fact was that the maximum yarn stiffness, E_{max}, was not constant at all three finenesses for zero twist level (and identical strain rates and specimen lengths). We remark that in equation (1) (which is needed for evaluation of equation (3)), we used the actual measured fineness (glass weight per length) and, therefore, the amount of resisting material was reflected correctly. Since the number of filaments was identical for all three yarn densities, the only source of difference could be the filament diameter (filaments of the different tex-numbers had the same shape of cross section, also the sizing was identical) and structural effects. Simply the 1200 tex yarn seemed to be more efficient with respect to glass amount than other tested types. This observation was supported by the fact that the 1200 tex yarn systematically achieved higher strengths.

It should be noted that interaction of the fineness and twist measured for the AR-glass yarns did not fit into the treatment provided by the standards [ASTM D885 Note 9, ASTM D 2256]. These standards handled the interaction due to slippage in the clamps and provided empirical formulae for twist levels to avoid it. The nature of **AD** interaction isolated here was different: the effect of fineness translated to the effect of filament diameter and the components were high-performance filaments with perfectly elastic and brittle behavior inducing different interaction mechanisms (fragmentation) compared to more flexible materials.

Conclusions

The multivariate study of continuous AR-glass multifilament yarns brought about an evidence of interaction between filaments through increase of bundle strength for a certain range of bundle twist. In particular, the study identified a significant effect of bond on the yarn performance for twist levels up to 20 turns/m. The increased filament-filament interaction could compensate for filament breaks during the loading and resulted in significantly higher bundle strength. We attributed this increase to the fragmentation of filaments in agreement with the description by Pan et al. [19]. However, as mentioned in the beginning, the strain homogenization along the filaments could also induce strength increase [17].

The question regarding which mechanism was responsible for the strength increase could only be addressed with the help of modeling. As the next step, the obtained data shall be interpreted with the help of available fiber bundle models to identify the dominating interaction mechanism and to extract the relevant parameters for configurations occurring in textile reinforced cementitious composites. Of particular interest is the quantification of the fragmentation density as a function of the lateral pressure.

As mentioned, the study was performed in the context of the research on textile-reinforced concrete exhibiting partial penetration of the yarn cross section. It should be emphasized that an improved performance of twisted yarns in tensile test cannot be reproduced in the composite. The reason for this is that twisting hinders the penetration of the matrix into the yarn with the consequence of lower outer bond. However, this was not the intention behind the present study. The twisting was imposed in order to study the bond between filaments and its interaction with lateral forces. These definitely occur in the composite, for example in the vicinity of crack bridges.

Acknowledgments

The work was supported by German Science Foundation under project numbers GR1311/13-1 and CH276/1-1. Additionally, the work of the second author was supported by the Czech Science Foundation (GACR grant no. 103/06/P086). This support is gratefully acknowledged.

Literature Cited

1. Swamy, R., and Hussin, M., Continuous Woven Polypropylene Mat Reinforced Cement Composites for Applications in Building Construction, in "Textile Composites in Building Construction," Pluralis, Paris, France, Part 1, pp. 55–67 (1990).
2. Meyer, C., and Vilkner, G., Glass Concrete Thin Sheets Prestressed with Aramid Fiber Mesh, in "Fourth International RILEM Workshop on High Performance Fiber Reinforced Cement Composites (HPFRCC4)," RILEM Publications SARL, Varenna, Italy, pp. 325–336 (2003).
3. Peled, A., and Bentur, A., Geometrical Characteristics and Efficiency of Textile Fabrics for Reinforcing Composites, *Cem. Concr. Res.* **30**(5), 781–790 (2000).
4. Chudoba, R., Vořechovský, M., and Konrad, M., Stochastic Modeling of Multi-filament Yarns I: Random Properties within the Cross Section and Size Effect, *Int. J. Solids Struct.* **43**(3–4), 413–434 (2006).
5. Vořechovský, M., and Chudoba, R., Stochastic Modeling of Multi-filament Yarns II: Random Properties Over the Length and Size Effect, *Int. J. Solids Struct.* **43**(3–4), 435–458 (2006).
6. Hegger, J., Will, N., and Bruckermann, O. S. V., Load-bearing Behavior and Simulation of Textile Reinforced Concrete, *Mater. Struct.* **39**(8), 765–775 (2006).
7. Banholzer, B., Tailoring of AR-glass Filament/Cement Based Matrix Bond – Analytical and Experimental Techniques, in "6th International RILEM Symposium on Fibre Reinforced Concretes," RILEM Publications SARL, Varenna, Italy, pp. 1443–1452 (2004).
8. Banholzer, B., "Bond Behaviour of a Multi-filament Yarn Embedded in a Cementitious Matrix," Institut für Bauforschung, RWTH Aachen, Aachen, Germany (2004).
9. Zhandarov, S., and Mäder, E., Characterization of Fiber/Matrix Interface Strength: An Applicability of Different Tests, Approaches and Parameters, *Compos. Sci. Technol.* **65**(1), 149–160 (2005).
10. Zhou, Y., Jiang, D., and Xia, Y., Tensile Mechanical Behavior of T300 and M40J Fiber Bundles at Different Strain Rate, *J. Mater. Sci.* **36**(4), 919–922 (2001).
11. Weibull, W., "The Phenomenon of Rupture in Solids," Royal Swedish Institute of Engineering Research (Ingenioersvetenskaps Akad Handl), Stockholm, Sweden, 153, pp. 1–55 (1939).
12. Peirce, F. T., Theorems on the Strength of Long and of Composite Specimens, *J. Textile Inst.* **17**, 355–368 (1926).
13. Phoenix, S. L., and Taylor, H. M., The Asymptotic Strength Distribution of a General Fiber Bundle, *Adv. Appl. Probab.* **5**, 200–216 (1973).
14. Daniels, H. E., The Statistical Theory of the Strength of Bundles of Threads, *Proc. R. Soc. Lond.* **183A**, 405 (1945).
15. Daniels, H. E., The Maximum of a Gaussian Process Whose Mean Path has a Maximum, with an Application to the Strength of Bundles of Fibres, *Adv. Appl. Probab.* **21**, 315–333 (1989).
16. Smith, R. L., The Asymptotic Distribution of a Series-parallel System with Equal Load-sharing, *Ann. Probab.* **10**(1), 137–171 (1982).
17. Hearle, J. W. S., Grosberg, P., and Backer, S., "Structural Mechanics of Fibers, Yarns, and Fabrics," Wiley-Interscience, New York, London, Sydney, Toronto (1969).
18. Phoenix, S. L., Statistical Theory for the Strength of Twisted Fiber Bundles with Applications to Yarns and Cables, *Textile Res. J.* **49**, 407–423 (1979).
19. Pan, N., Hua, T., and Qiu, Y., Relationship Between Fiber and Yarn Strength, *Textile Res. J.* **71**(11), 960–964 (2001).
20. Broughton, R. M., Mogahzy, Y. E., and Hall, D. M., Mechanism of Yarn Failure, *Textile Res. J.* **92**(3), 131–134 (1992).
21. Realff, M. L., Pan, N., Seo, M., Boyce, C. M., A Stochastic Simulation of the Failure Process and Ultimate Strength of Blended Continuous Yarns, *Textile Res. J.* **70**(5), 415–430 (2000).
22. Jones, J. E., Haddad, G. N., and Sutton, J. E., Tensile Characteristics of Twisted Continuous-filament Glass Yarns, *Textile Res. J.* **41**(11), 900–904 (1971).
23. Haddad, G. N., and Sutton, J. E., Application of the Law of Composites to Twisted Continuous-filament Glass/Nylon Blended Yarns, *Textile Res. J.* **42**(8), 452–459 (1972).
24. Rao, Y., and Farris, R. J., A Modeling and Experimental Study of the Influence of Twist on the Mechanical Properties of High-performance Fiber Yarns, *J. Appl. Polym. Sci.* **77**(9), 1938–1949 (2000).
25. Montgomery, D. C., "Design and Analysis of Experiments," John Wiley and Sons Inc. (2001).
26. Lam, J. K. C., and Postle, R., Multivariate Studies of Mechanical Properties for Wool and Cotton Fabrics, *Textile Res. J.* **76**(5), 414–425 (2006).
27. Dean, A., and Voss, D., "Design and Analysis of Experiments," Springer-Verlag (1999).